Composites: Part B 44 (2013) 84–94

Contents lists available at SciVerse ScienceDirect

Composites: Part B

journal homepage: www.elsevier.com/locate/compositesb

Nonlocal buckling of double-nanoplate-systems under biaxial compression

T. Murmu [a,*], J. Sienz [b], S. Adhikari [b], C. Arnold [b]

[a] Mechanical, Aeronautical and Biomedical Engineering, University of Limerick, Ireland
[b] College of Engineering, Swansea University, Singleton Park, Swansea SA2 8PP, Wales, UK

ARTICLE INFO

Article history:
Received 18 January 2012
Received in revised form 6 June 2012
Accepted 7 July 2012
Available online 22 August 2012

Keywords:
A. Nano-structures
B. Buckling
C. Analytical modelling
Nonlocal elasticity

ABSTRACT

This paper reports an analytical study on the buckling of double-nanoplate-system (DNPS) subjected to biaxial compression using nonlocal elasticity theory. The two nanoplates of DNPS are bonded by an elastic medium. Nonlocal plate theory is utilized for deriving the governing equations. An analytical method is used for determining the buckling load of DNPS under biaxial compression. Difference between nonlocal uniaxial and biaxial buckling in DNPS is shown. Both synchronous and asynchronous buckling phenomenon of biaxially compressed DNPS is highlighted. Study shows that the small-scale effects in biaxially compressed DNPS increases with increasing values of nonlocal parameter for the case of synchronous modes of buckling than in the asynchronous modes of buckling. The buckling load decrease with increase of value of nonlocal parameter or scale coefficient. In biaxial compression higher buckling modes are subjected to higher nonlocal effects in DNPS. Further the study shows that the increase of stiffness parameter brings uniaxial and biaxial buckling phenomenon closer while increase of aspect ratio widen uniaxial and biaxial buckling phenomenon.

1. Introduction

Nanoplates are two-dimensional structure of nano-scale size. Researches on the nanoplates are increasing every day. Popular nanoplates which are experimentally and computationally studied include monolayer graphene [1] and multi-layer graphene sheets (GS). Other nanoplates capturing attention among scientific community are gold nanoplates [2–4], silver nanoplates [5,6], ZnO nanoplates [7] and boron-nitride sheets [8,9]. These nanoplates possess superior properties over traditional engineering materials. Nanoplates such as GS are being found in potential application areas such as in nano-electronic mechanical-systems (NEMS) [10], nanosensors [11], nanoactuators [12], transistor [13,14], solar cells [15–17], biomedical [18], space elevator lifts in the form of nanoribbons and in nanocomposites.

One important technological advancement to the concept of the single or mono nanoplates [19] is that of the complex-nanoplate-systems. The complex nanoplates can be considered as composite nanostructure. The composite nanostructure can be developed according to specific structural and physical requirements. Structural requirements may include developing advanced nanocomposites where nanoplates are coupled by bonding resins. One simple example of complex-nanoplate-system is the double-nanoplate-system (DNPS) [20]. DNPS are two nanoplates bonded by elastic medium such as polymer resin. The elastic medium is generally modelled as Winkler springs. It should be noted that the present DNPS are different from double-layered system, such as double-walled graphene systems [21]. These double-walled nanoentities are generally bonded by a constant van der Waal force which is unlike the double-nanobeam-system or double-nanoplate-system. DNPS would have different bonding agent of varying stiffness modulus.

zDNPS bonded by an elastic medium can be observed in nanocomposites. Vibration and buckling study of DNPS would thus be important in-line with the similar studies on single-layer nanoplates. The DNPS can also be developed as a sandwich structure where the connecting elastic substance could be soft and light weight, and considered to be the core. The composite sandwich would have potential to be used in microelectromechanical systems (MEMS) and nanoelectromechanical systems (NEMS). Buckling would therefore be one of the important behaviour of nanosandwich plate subjected to in-plane compressive forces. The mechanical in-stability study of sandwich DNPS as double-layer graphene optical modulator [22] would also be important. The analysis on long DNPS could also be useful for design and development of nano-optomechanical systems (NOMS) [23]. Recently Murmu and Adhikari [20,24] and Pouresmaeeli et al. [25] has carried out buckling and vibration analysis of DNPS.

Literature shows that research on size-dependent structural theories [26–29] are becoming increasing common for more accurate design and analysis of micro and nanostructures. Though molecular dynamic (MD) simulation is justified for the analysis of nanostructure the approach is computationally exorbitant for

* Corresponding author.
E-mail address: murmutony@gmail.com (T. Murmu).

1359-8368/$ - see front matter © 2012 Elsevier Ltd. All rights reserved.
http://dx.doi.org/10.1016/j.compositesb.2012.07.053

nanostructures with large numbers of atoms. This asks for the use of conventional continuum mechanics in analysis of nanostructures. Classical continuum modelling approach is considered scale-free. It lacks the accountability of the effects arising from the small-scale where size-effects are prominent. Nanoscale experiments demonstrate that the mechanical properties of nano-dimensional materials are much influenced by the size-effects or scale-effects. Size-effects are related to atoms and molecules that constitute the materials. The application of classical continuum approaches may be thus questionable in the analysis of nanostructures such as nanorods, nanobeams and nanoplates.

One widely promising size-dependant continuum theory is the nonlocal elasticity theory pioneered by Eringen [30] which brings in the size-effects or scale-effects and underlying physics within the formulation. Nonlocal elasticity theory contains information related to the forces between atoms, and the internal length scale in structural, thermal and mechanical analysis. In the nonlocal elasticity theory, the small-scale effects are captured by assuming that the stress at a point is a function of the strains at all points in the domain. Literature would show that numerous motivating works of nanostructures based on nonlocal elasticity has been reported [21,31–61]. Nonlocal theory considers long-range inter-atomic interaction and yields results dependent on the size of a body.

Since DNPS would be important as structural nanocomponents, the study and understanding of its mechanical vibration and buckling phenomenon are necessary. Compared to study on uniaxial buckling, the biaxial buckling phenomenon of DNPS has received very little attention. Recently Murmu and Pradhan [62] and Pradhan and Murmu [63] carried out study of biaxial buckling of single-layered nanoplates. According to the author's knowledge, till date, the study on biaxial buckling phenomenon of DNPS is absent in literature. This paper addresses the biaxial buckling behavioural phenomenon of double-nanoplate-systems [20] under the umbrella of nonlocal elasticity. In the present problem, the nanoplates are considered as single-layer graphene sheets. The present study can be used beyond graphene sheets as nanoplates. The two single-layered graphene sheets are elastically connected by enclosing elastic medium such as polymer resin modelled as springs. Expressions for biaxial buckling load of system are derived using nonlocal elasticity theory [30]. Explicit closed-form expressions for buckling load are derived for the case when all four ends are simply-supported. Further, this paper presents a unique yet simple method of obtaining the exact solution for the buckling load of biaxially compressed double-graphene-sheet-system. Attention is put on the nonlocal scale effects in synchronous and asynchronous modes of buckling for various coupling springs, aspect ratio, higher buckling loads and compression ratios. Hopefully present study is expected to bring about understanding into the inside of buckling behaviour of biaxially compressed double-nanoplates-systems.

2. Nonlocal elasticity theory

In this section we provide concise fundamentals of nonlocal elasticity. In nonlocal elasticity theory [30], the basic equations for an isotropic linear homogenous nonlocal elastic body neglecting the body force are given as

$$\begin{aligned} &\sigma_{ij,i} = 0 \\ &\sigma_{ij}(x) = \int_V \phi(|x-x'|,\alpha) t_{ij} dV(x'), \quad \forall x \in V \\ &t_{ij} = H_{ijkl}\varepsilon_{kl} \\ &\varepsilon_{ij} = \frac{1}{2}(u_{i,j} + u_{j,i}) \end{aligned} \tag{1}$$

The terms σ_{ij}, t_{ij}, ε_{kl}, H_{ijkl} represents nonlocal stress, classical stress, classical strain and fourth order elasticity tensors respectively. The volume integral is over the region V occupied by the body. The kernel function $\phi(|x-x'|,\alpha)$ denotes the nonlocal modulus. The nonlocal modulus acts as an attenuation function incorporating into constitutive equations the nonlocal effects at the reference point x produced by local strain at the source x'. The term $|x-x'|$ represents the distance in the Euclidean form and α is a material constant that depends on the internal characteristics length, a (e.g. lattice parameter, granular size, distance between the C–C bonds) and external characteristics length, ℓ (e.g. crack length, wave length). Material constant α is defined as $\alpha = e_0 a/\ell$ where e_0 is a constant for calibrating the model with experimental results or other validated models (molecular dynamics). According to Eringen [30], the value of e_0 is reported as 0.39. The parameter e_0 is estimated such that the relations of the nonlocal elasticity model could provide satisfactory approximation to the atomic dispersion curves of the plane waves with those obtained from the atomistic lattice dynamics.

3. Governing equations of biaxially compressed DNPS

Nonlocal integral equation (Eq. (1)) is in partial–integral form and generally difficult to solve analytically [30]. Thus a differential form of nonlocal elasticity equation is often used. The nonlocal constitutive stress–strain relation can be simplified as

$$(1-\alpha^2\ell^2\nabla^2)\sigma_{ij} = t_{ij} \tag{2}$$

where ∇^2 is the Laplacian.

Utilising the differential equation form of nonlocal elasticity (Eq. (2)) we develop the equations for buckling phenomenon of biaxial compressed DNPS [20]. We refer the two typical nanoplates in DNPS as nanoplate-1 and nanoplate-2 as shown in Fig. 1. The two nanoplates of DNPS are bonded by an elastic medium such as polymer resin. The elastic medium between two nanoplates is represented by vertically distributed identical springs. The springs are oriented perpendicular to the nanoplates. The springs are assumed to have a stiffness k. Different value of k for different polymer matrix (elastic medium) can be used for the study. The nanoplates are considered to be of length L and width W. Generally, the two nanoplates are different where the length, width, and bending rigidity of the ith plate are L_i, W_i, and D_i ($i = 1, 2$) respectively. These parameters are assumed to be constant along each nanoplate.

We assume that the two nanoplates of DNPS are biaxially compressed. N_{x1} and N_{y1} denote the two biaxial compressive forces in x and y directions respectively acting on nanoplate-1 (Fig. 1). While N_{x2} and N_{y2} denote the two biaxial forces in x and y directions respectively acting on nanoplate-2. The bending displacements over the two nanoplates for the buckling analysis are denoted by $w_1(x,y)$ and $w_2(x,y)$. The individual governing equations of the nanoplates (nanoplate-1 and nanoplate-2) under biaxial compression based on nonlocal plate theory [40,55,64–66] can be written as

Nanoplate-1:

$$\begin{aligned} &D_1\left(\frac{\partial^4 w_1(x,y)}{\partial x^4} + 2\frac{\partial^4 w_1(x,y)}{\partial x^2\partial y^2} + \frac{\partial^4 w_1(x,y)}{\partial y^4}\right) + k[w_1(x,y) - w_2(x,y)] \\ &- k(e_0a)^2\left(\frac{\partial^2}{\partial x^2} + \frac{\partial^2}{\partial y^2}\right)[w_1(x,y) - w_2(x,y)] - N_{x1}\frac{\partial^2 w_1(x,y)}{\partial x^2} \\ &+ N_{x1}(e_0a)^2\left(\frac{\partial^2}{\partial x^2} + \frac{\partial^2}{\partial y^2}\right)\frac{\partial^2 w_1(x,y)}{\partial x^2} - N_{y1}\frac{\partial^2 w_1(x,y)}{\partial y^2} \\ &+ N_{y1}(e_0a)^2\left(\frac{\partial^2}{\partial x^2} + \frac{\partial^2}{\partial y^2}\right)\frac{\partial^2 w_1(x,y)}{\partial y^2} = 0 \end{aligned} \tag{3}$$

where the bending rigidity of nanoplate-1 is expressed as

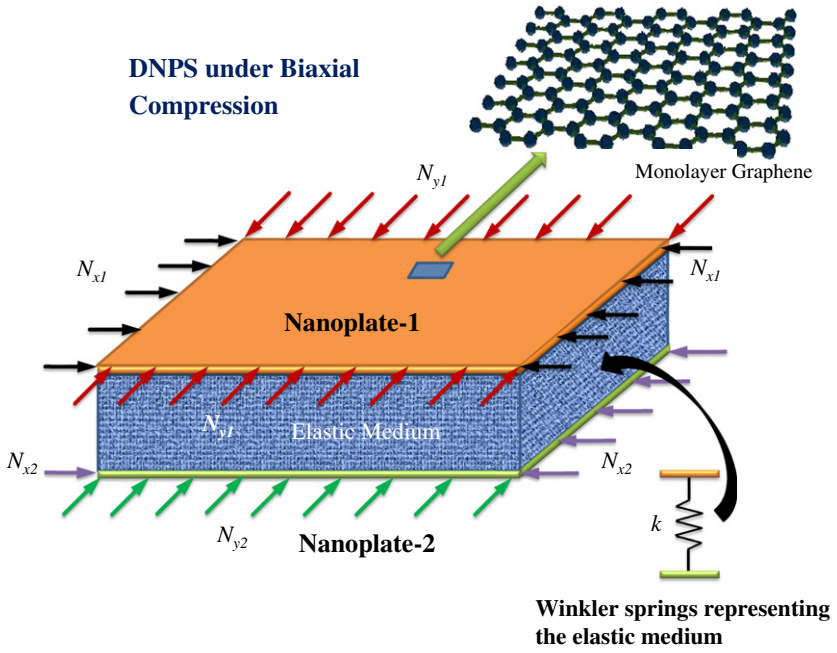

Fig. 1. Schematic diagram of double-nanoplate-systems (DNPS) subjected to biaxial compression.

$$D_1 = E_1 h_1^3/12(1-\vartheta_1^2) \tag{4}$$

Here the terms E, h, ϑ in Eq. (4) denote the Young's modulus, thickness and the Poisson's ratio of the nanoplates.

Nanoplate-2:

$$\begin{aligned} &D_2\left(\frac{\partial^4 w_2(x,y)}{\partial x^4}+2\frac{\partial^4 w_2(x,y)}{\partial x^2\partial y^2}+\frac{\partial^4 w_2(x,y)}{\partial y^4}\right)-k[w_1(x,y)\\ &-w_2(x,y)]+k(e_0a)^2\left(\frac{\partial^2}{\partial x^2}+\frac{\partial^2}{\partial y^2}\right)[w_1(x,y)-w_2(x,y)]-N_{x2}\\ &\times\frac{\partial^2 w_2(x,y)}{\partial x^2}+N_{x2}(e_0a)^2\left(\frac{\partial^2}{\partial x^2}+\frac{\partial^2}{\partial y^2}\right)\frac{\partial^2 w_2(x,y)}{\partial x^2}-N_{y2}\\ &\times\frac{\partial^2 w_2(x,y)}{\partial y^2}+N_{y2}(e_0a)^2\left(\frac{\partial^2}{\partial x^2}+\frac{\partial^2}{\partial y^2}\right)\frac{\partial^2 w_2(x,y)}{\partial y^2}\\ &=0 \end{aligned} \tag{5}$$

where the bending rigidity of nanoplate-2 is expressed as

$$D_2 = E_2 h_2^3/12(1-\vartheta_2^2) \tag{6}$$

It should be noticed that when the nonlocal parameter (which considers the scale effects) is neglected ($e_0a = 0$), Eqs. (3) and (5) reverts back to classical plate equations. For derivation of nonlocal plate theory one can refer [67].

Let us define the relation between biaxial compression ratios of two nanoplates as

$$\delta_1 = \frac{N_{y1}}{N_{x1}} \tag{7}$$

$$\delta_2 = \frac{N_{y2}}{N_{x2}} \tag{8}$$

Substituting Eqs. (7) and (8), the individual equation of nanoplates (Eqs. (3) and (5)) reduces to

Nanoplate-1:

$$\begin{aligned} &D_1\left(\frac{\partial^4 w_1(x,y)}{\partial x^4}+2\frac{\partial^4 w_1(x,y)}{\partial x^2\partial y^2}+\frac{\partial^4 w_1(x,y)}{\partial y^4}\right)+k[w_1(x,y)\\ &-w_2(x,y)]-k(e_0a)^2\left(\frac{\partial^2}{\partial x^2}+\frac{\partial^2}{\partial y^2}\right)[w_1(x,y)-w_2(x,y)]\\ &-N_{x1}\left(\frac{\partial^2 w_1(x,y)}{\partial x^2}+\delta_1\frac{\partial^2 w_1(x,y)}{\partial y^2}\right)\\ &+(e_0a)^2N_{x1}\left[\frac{\partial^4 w_1(x,y)}{\partial x^4}+(\delta_1+1)\frac{\partial^4 w_1(x,y)}{\partial x^2\partial y^2}+\delta\frac{\partial^4 w_1(x,y)}{\partial y^4}\right]\\ &=0 \end{aligned} \tag{9}$$

Nanoplate-2:

$$\begin{aligned} &D_2\left(\frac{\partial^4 w_2(x,y)}{\partial x^4}+2\frac{\partial^4 w_2(x,y)}{\partial x^2\partial y^2}+\frac{\partial^4 w_2(x,y)}{\partial y^4}\right)-k[w_1(x,y)\\ &-w_2(x,y)]+k(e_0a)^2\left(\frac{\partial^2}{\partial x^2}+\frac{\partial^2}{\partial y^2}\right)[w_1(x,y)-w_2(x,y)]\\ &-N_{x2}\left(\frac{\partial^2 w_2(x,y)}{\partial x^2}+\delta_2\frac{\partial^2 w_2(x,y)}{\partial y^2}\right)\\ &+(e_0a)^2N_{x2}\left[\frac{\partial^4 w_2(x,y)}{\partial x^4}+(\delta_2+1)\frac{\partial^4 w_2(x,y)}{\partial x^2\partial y^2}+\delta\frac{\partial^4 w_2(x,y)}{\partial y^4}\right]\\ &=0 \end{aligned} \tag{10}$$

In this paper we consider the properties of the two nanoplates as identical:

$$D_1 = D_2 = D \equiv \text{constant} \tag{11}$$

And the loading conditions and the compression ratios in the nanoplates are considered as

$$N_{x1} = N_{x2} = N_x \tag{12}$$

$$\delta_1 = \delta_2 = \delta \tag{13}$$

The incorporation of the above assumptions simplifies the solution of the problem.

Substituting the assumptions (Eqs. (11)–(13)) in Eqs. (9) and (10) we get

Nanoplate-1:

$$\begin{aligned}
&D\left(\frac{\partial^4 w_1(x,y)}{\partial x^4} + 2\frac{\partial^4 w_1(x,y)}{\partial x^2 \partial y^2} + \frac{\partial^4 w_1(x,y)}{\partial y^4}\right) + k[w_1(x,y) \\
&- w_2(x,y)] - k(e_0a)^2\left(\frac{\partial^2}{\partial x^2} + \frac{\partial^2}{\partial y^2}\right)[w_1(x,y) - w_2(x,y)] \\
&- N_x\left(\frac{\partial^2 w_1(x,y)}{\partial x^2} + \delta\frac{\partial^2 w_1(x,y)}{\partial y^2}\right) \\
&+ (e_0a)^2 N_x\left[\frac{\partial^4 w_1(x,y)}{\partial x^4} + (\delta+1)\frac{\partial^4 w_1(x,y)}{\partial x^2 \partial y^2} + \delta\frac{\partial^4 w_1(x,y)}{\partial y^4}\right] \\
&= 0
\end{aligned} \tag{14}$$

Nanoplate-2:

$$\begin{aligned}
&D\left(\frac{\partial^4 w_2(x,y)}{\partial x^4} + 2\frac{\partial^4 w_2(x,y)}{\partial x^2 \partial y^2} + \frac{\partial^4 w_2(x,y)}{\partial y^4}\right) - k[w_1(x,y) \\
&- w_2(x,y)] + k(e_0a)^2\left(\frac{\partial^2}{\partial x^2} + \frac{\partial^2}{\partial y^2}\right)[w_1(x,y) - w_2(x,y)] \\
&- N_x\left(\frac{\partial^2 w_2(x,y)}{\partial x^2} + \delta_1\frac{\partial^2 w_2(x,y)}{\partial y^2}\right) \\
&+ (e_0a)^2 N_x\left[\frac{\partial^4 w_2(x,y)}{\partial x^4} + (\delta+1)\frac{\partial^4 w_2(x,y)}{\partial x^2 \partial y^2} + \delta\frac{\partial^4 w_2(x,y)}{\partial y^4}\right] \\
&= 0
\end{aligned} \tag{15}$$

For the solution of Eqs. (14) and (15), we apply a change of variables by considering w as the relative displacement of the nanoplate-1 with respect to the nanoplate-2 such as [20]

$$w(x,y) = w_1(x,y) - w_2(x,y) \tag{16}$$

such that for nanoplate-1, the displacement is expressed as

$$w_1(x,y) = w(x,y) + w_2(x,y) \tag{17}$$

Subtracting Eq. (14) from (15) would lead to

$$\begin{aligned}
&D\left(\frac{\partial^4[w_1(x,y) - w_2(x,y)]}{\partial x^4} + 2\frac{\partial^4[w_1(x,y) - w_2(x,y)]}{\partial x^2 \partial y^2} + \frac{\partial^4[w_1(x,y) - w_2(x,y)]}{\partial y^4}\right) \\
&+ 2k[w_1(x,y) - w_2(x,y)] - 2k(e_0a)^2\left(\frac{\partial^2}{\partial x^2} + \frac{\partial^2}{\partial y^2}\right)[w_1(x,y) - w_2(x,y)] \\
&- N_x\left(\frac{\partial^2[w_1(x,y) - w_2(x,y)]}{\partial x^2} + \delta\frac{\partial^2[w_1(x,y) - w_2(x,y)]}{\partial y^2}\right) \\
&+ (e_0a)^2 N_x\left[\frac{\partial^4[w_1(x,y) - w_2(x,y)]}{\partial x^4} + (\delta+1)\frac{\partial^4[w_1(x,y) - w_2(x,y)]}{\partial x^2 \partial y^2}\right. \\
&\left.+\delta\frac{\partial^4[w_1(x,y) - w_2(x,y)]}{\partial y^4}\right] = 0
\end{aligned} \tag{18}$$

Utilising Eq. (16) in Eqs. (14) and (15) we get

$$\begin{aligned}
&D\left(\frac{\partial^4 w(x,y)}{\partial x^4} + 2\frac{\partial^4 w(x,y)}{\partial x^2 \partial y^2} + \frac{\partial^4 w(x,y)}{\partial y^4}\right) + 2kw(x,y) \\
&- 2k(e_0a)^2\left(\frac{\partial^2 w(x,y)}{\partial x^2} + \frac{\partial^2 w(x,y)}{\partial y^2}\right) \\
&- N_x\left(\frac{\partial^2 w(x,y)}{\partial x^2} + \delta\frac{\partial^2 w(x,y)}{\partial y^2}\right) \\
&+ (e_0a)^2 N_x\left[\frac{\partial^4 w(x,y)}{\partial x^4} + (\delta+1)\frac{\partial^4 w(x,y)}{\partial x^2 \partial y^2} + \delta\frac{\partial^4 w(x,y)}{\partial y^4}\right] \\
&= 0
\end{aligned} \tag{19}$$

and

$$\begin{aligned}
&D\left(\frac{\partial^4 w_2(x,y)}{\partial x^4} + 2\frac{\partial^4 w_2(x,y)}{\partial x^2 \partial y^2} + \frac{\partial^4 w_2(x,y)}{\partial y^4}\right) \\
&- N_x\left(\frac{\partial^2 w_2(x,y)}{\partial x^2} + \delta\frac{\partial^2 w_2(x,y)}{\partial y^2}\right) \\
&+ (e_0a)^2 N_x\left[\frac{\partial^4 w_2(x,y)}{\partial x^4} + (\delta+1)\frac{\partial^4 w_2(x,y)}{\partial x^2 \partial y^2} + \delta\frac{\partial^4 w_2(x,y)}{\partial y^4}\right] \\
&= kw(x,y) - k(e_0a)^2\left(\frac{\partial^2 w(x,y)}{\partial x^2} + \frac{\partial^2 w(x,y)}{\partial y^2}\right)
\end{aligned} \tag{20}$$

For the present analysis of coupled DNPS, we see the simplicity in using Eqs. (19) and (20). It should be noted that when the nonlocal effects are ignored ($e_0a = 0$) and a single nanoplate is considered, the above equations revert to the equations of double-plate-system based on classical Kirchhoff's plate theory.

Now we present the mathematical expressions of the boundary conditions of the DNPS. It is assumed that all the edges in the nanoplate system simply-supported. The use of boundary conditions is described here. At each ends of the nanoplates in DNPS the displacement and the nonlocal moments are considered to be zero. They can be mathematically expressed as

Nanoplate-1:

Displacement condition:

$$w_1(0,y) = 0; \quad w_1(L,y) = 0; \quad w_1(x,0) = 0; \quad w_1(x,W) = 0; \tag{21}$$

Nonlocal moment condition:

$$M_1(0,y) = 0; \quad M_1(L,y) = 0; \quad M_1(x,0) = 0; \quad M_1(x,W) = 0; \tag{22}$$

Nanoplate-2:Displacement condition:

$$w_2(0,y) = 0; \quad w_2(L,y) = 0; \quad w_2(x,0) = 0; \quad w_2(x,W) = 0; \tag{23}$$

Nonlocal moment condition:

$$M_2(0,y) = 0; \quad M_2(L,y) = 0; \quad M_2(x,0) = 0; \quad M_2(x,W) = 0; \tag{24}$$

Now we use Eq. (16) in the displacement boundary Conditions (21) and (23),

$$w(0,y) = w_1(0,y) - w_2(0,y) = 0 \tag{25a}$$
$$w(L,y) = w_1(L,y) - w_2(L,y) = 0 \tag{25b}$$
$$w(x,0) = w_1(x,0) - w_2(x,0) = 0 \tag{25c}$$
$$w(x,W) = w_1(x,W) - w_2(x,W) = 0 \tag{25d}$$

Similarly using Eq. (16) in the nonlocal moment boundary Conditions (22) and (24),

$$M(0,y) = M_1(0,y) - M_2(0,y) = 0 \tag{26a}$$
$$M(L,y) = M_1(L,y) - M_2(L,y) = 0 \tag{26b}$$
$$M(x,0) = M_1(x,0) - M_2(x,0) = 0 \tag{26c}$$
$$M(x,W) = M_1(x,W) - M_2(x,W) = 0 \tag{26d}$$

4. Buckling loads of biaxially compressed DNPS

In this section different explicit cases of nonlocal biaxial buckling will be considered. The nanoplate system is subjected to both uniaxial as well as biaxial compressive forces. The cases studied will be nanoplates buckling with out-of-phase (asynchronous); in-phase (synchronous); and when one of the nanoplates is considered to be fixed.

The double-nanoplate-system is assumed to be bi-axially buckled. Fig. 2 shows the three dimensional configuration of double-nanoplate-system with the asynchronous (out-of-phase) sequence of buckling ($w_1 - w_2 \neq 0$). It should be noted that the figure represents first out-of-phase buckling phenomenon not the first buckled mode. In out-of-phase, sequence of buckling the nanoplates is buckled in opposite directions.

We evaluate the buckling load for the out-of-phase (asynchronous) type buckling. We use Eq. (19) for the biaxial buckling solution of double-nanoplate-system.

We assume that the buckling mode of the double-nanoplate-system as

$$w(x,y) = W_{mn} \sin\frac{m\pi x}{L} sin\frac{n\pi y}{W} \tag{27}$$

where m and n are the half wave number.

Substituting Eq. (27) into Eq. (19) and simplifying we get

$$\begin{aligned} &D\left[\left(\frac{m\pi}{L}\right)^4 + 2\left(\frac{m\pi}{L}\right)^2\left(\frac{n\pi}{W}\right)^2 + \left(\frac{n\pi}{W}\right)^4\right]w + 2kw \\ &+ 2k(e_0a)^2\left[\left(\frac{m\pi}{L}\right)^2 + \left(\frac{n\pi}{W}\right)^2\right]w + N_x\left[\left(\frac{m\pi}{L}\right)^2 + \delta\left(\frac{n\pi}{W}\right)^2\right]w \\ &+ (e_0a)^2N_x\left[\left(\frac{m\pi}{L}\right)^4 + (\delta+1)\left(\frac{m\pi}{L}\right)^2\left(\frac{n\pi}{W}\right)^2 + \delta\left(\frac{n\pi}{W}\right)^4\right]w \\ &= 0 \end{aligned} \tag{28}$$

For the sake of simplicity, we utilise the following parameters

$$K = \frac{kL^4}{D}; \quad \widehat{N} = -\frac{N_xL^2}{D}; \quad \mu = \frac{e_0a}{L}; \quad R = \frac{L}{W} \tag{29}$$

Substituting Eq. (29) into Eq. (28) yields the biaxial buckling load expression for asynchronous modes:

$$\widehat{N}_{\text{Asyn}} = \frac{[(m\pi)^4 + 2R^2(m\pi)^2(n\pi)^2 + R^4(n\pi)^4] + 2K + 2K\mu^2[(m\pi)^2 + R^2(n\pi)^2]}{((m\pi)^2 + \delta R^2(n\pi)^2 + \mu^2[(m\pi)^4 + R^2(\delta+1)(m\pi)^2(n\pi)^2 + \delta R^4(n\pi)^4])} \tag{30}$$

In-phase (synchronous) sequence type of buckling of the DNPS under bi-axial compression is also being considered here. The schematic illustration buckling is shown in Fig. 3, which is the first mode synchronous type buckling. In synchronous buckling both the nanoplates buckle in the same direction. For the present nanoplate system, the relative displacements between the two nanoplates are absent i.e. ($w_1 - w_2 = 0$). In synchronous buckling state,

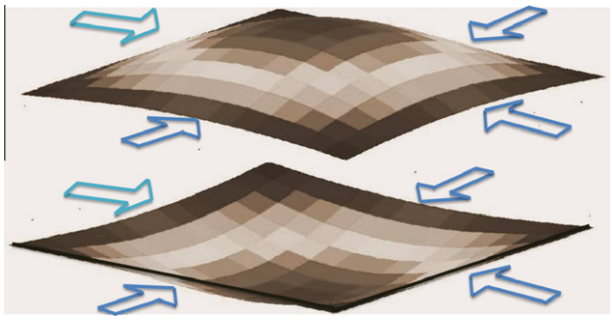

Fig. 2. Asynchronous-type bi-axial buckling.

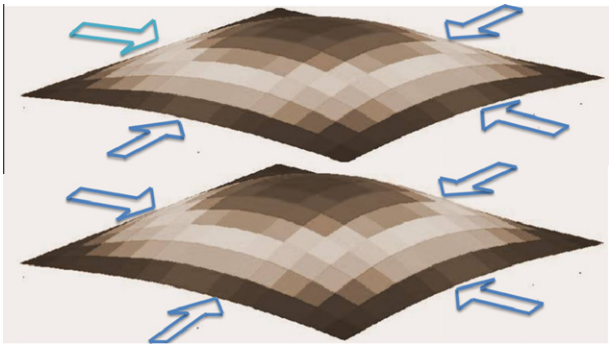

Fig. 3. Synchronous-type bi-axial buckling.

the double-nanoplate-system can be considered to be as one of the nanoplate (viz. nanoplate-2). Here we solve Eq. (20) for the synchronous sequence of buckling. We apply the same procedure as earlier for solving Eq. (19). The buckling load of the nonlocal double-nanoplate-system can be evaluated as

$$\widehat{N}_{\text{Syn}} = \frac{[(m\pi)^4 + 2R^2(m\pi)^2(n\pi)^2 + R^4(n\pi)^4]}{((m\pi)^2 + \delta R^2(n\pi)^2 + \mu^2[(m\pi)^4 + R^2(\delta+1)(m\pi)^2(n\pi)^2 + \delta R^4(n\pi)^4])} \tag{31}$$

Here we see for this case, the buckling phenomenon in the double-nanoplate-system is independent of the stiffness of the coupling springs and therefore the DNPS undergoing biaxial compression can be effectively treated as a single nanoplate.

Consider the case of DNPS when one of the two nanoplates (viz. nanoplate-2) is stationary ($w_2 = 0$). The schematic configuration of the NDNPS is shown in Fig. 4. Here the buckling phenomenon happens in nanoplate-1 only. We utilise the equations from nonlocal elasticity, and the governing equation for the DNPS in this case reduces to:

$$\begin{aligned} &D\left(\frac{\partial^4 w(x,y)}{\partial x^4} + 2\frac{\partial^4 w(x,y)}{\partial x^2\partial y^2} + \frac{\partial^4 w(x,y)}{\partial y^4}\right) + kw \\ &- k(e_0a)^2\left(\frac{\partial^2 w(x,y)}{\partial x^2} + \frac{\partial^2 w(x,y)}{\partial y^2}\right) \\ &- N_x\left(\frac{\partial^2 w(x,y)}{\partial x^2} + \delta\frac{\partial^2 w(x,y)}{\partial y^2}\right) \\ &+ (e_0a)^2N_x\left[\frac{\partial^4 w(x,y)}{\partial x^4} + (\delta+1)\frac{\partial^4 w(x,y)}{\partial x^2\partial y^2} + \delta\frac{\partial^4 w(x,y)}{\partial y^4}\right] \\ &= 0 \end{aligned} \tag{32}$$

Here it is worth noting that in this case, the DNPS behaves as if nanoplate embedded or supported on an elastic medium or other forces in nanoscale (Fig. 4). The elastic medium can be modelled as Winkler elastic foundation or Pasternak foundation. The stiffness of the elastic medium is denoted by k. By following the same procedure as solution of Eq. (19), the explicit nonlocal buckling load of biaxially compressed DNPS can be easily obtained. The buckling load is evaluated as

$$\widehat{N} = \frac{[(m\pi)^4 + 2R^2(m\pi)^2(n\pi)^2 + R^4(n\pi)^4] + K + K\delta^2[(m\pi)^2 + R^2(n\pi)^2]}{((m\pi)^2 + \delta R^2(n\pi)^2 + \mu^2[(m\pi)^4 + R^2(\delta+1)(m\pi)^2(n\pi)^2 + \delta R^4(n\pi)^4])} \tag{33}$$

When the nonlocal effects are ignored ($\mu = 0$ the above Eq. (33) reverts to that of local buckling phenomenon. In fact when one of the nanoplate (viz. nanoplate-2) in DNPS is fixed ($w_2 = 0$), the DNPS behaves as nanoplate on an elastic medium.

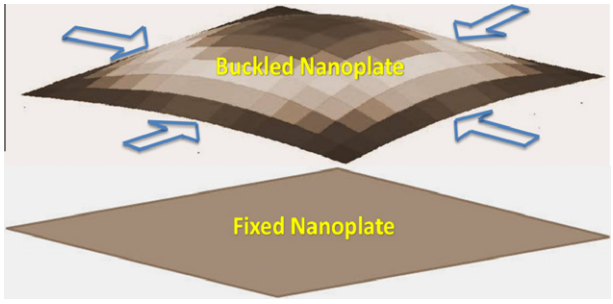

Fig. 4. Bi-axial buckling with one nanoplate fixed.

5. Result and discussions

5.1. Molecular dynamics vs. nonlocal plate theory

In literature, nonlocal plate theory has been compared with the molecular dynamics simulation. However the reliability of the theory depends on the value of nonlocal parameter. Details on the various values of nonlocal parameter as reported by various researchers is discussed in [68]. Molecular dynamics (MD) simulations for the free vibration of various graphene sheets using nonlocal plate theory with different values of side length and chirality can be found equivalent to the nonlocal plate model [64]. Using some optimised nonlocal parameter, the nonlocal plate model can predict the resonant frequencies with great accuracy. Further it is also shown that the nonlocal plate models as compared with molecular dynamics simulation can provide a remarkably accurate prediction of the graphene sheet behaviour under nonlinear vibration in thermal environments [69]. Thus nonlocal plate theory can be a reliable theory to predict the mechanical behaviour of nanoplates considering that optimised nonlocal parameter or scale coefficient is used.

5.2. Biaxial compressed coupled-graphene-sheet-system

For illustration, the properties of the nanoplates in DNPS are considered that of a single-walled graphene sheets. In the present work, lattice structure of graphene at small scale is addressed by the nonlocal elasticity theory. The two graphene sheets (GS) are coupled by the polymer matrix. Here it should be noted that the double-graphene-sheet-system is different from the double-walled-graphene-sheet. The bonded double-graphene-sheet-system is biaxially compressed by external forces. The effective properties of GS are considered. The Young's modulus of the GS is assumed as $E = 1.06$ TPa, density $\rho = 2300$ kg/m^3, the Poisson's ratio $\vartheta = 0.25$. The thickness of the GS is taken as $h = 0.34$ nm. The nonlocal double-plate theory for biaxially compressed DNPS illustrated here is a generalised theory and can be applied for the buckling analysis of coupled graphene sheets (multiple-walled), gold nanoplates, silver nanoplates, boron nitride sheets, etc. For generality, the buckling solutions of the DNPS are presented in terms of the buckling load parameter. The buckling load parameter is normalised buckling load and is considered as

$$\text{Buckling load parameter} = \frac{\text{Buckling load} \times L^2}{D} \tag{34}$$

The nonlocal parameter and the stiffness of the springs are computed as given in Eq. (29). Different values of spring parameters, K, are considered. Spring stiffness represents the stiffness of the enclosing elastic medium. Both high and large stiffness of springs are assumed. Values of K range from 5 to 50. Both the graphene sheets (GS-1 and GS-2) are assumed to have the same geometrical and material properties. In the present study we take the scale coefficient or nonlocal parameter in the range as $\mu = 0$–1, as specific value of nonlocal parameter of double graphene system is matter of open research.

5.3. Effect of small-scale parameter on biaxially compressed DNPS

To see the influence of small-scale on the natural buckling load of the coupled-graphene sheet-systems subjected to bi-axial loading, curves have been plotted for buckling load parameter and scale coefficient (nonlocal parameter). The variation of the buckling load parameter with the change in scale coefficient is shown in Fig. 5. Square nanoplates of edge 5 nm are considered for the DNPS. The stiffness parameter of the coupling springs between the nanoplates is assumed to be constant ($K = 20$). Both phenomenon of structural buckling is concerned, i.e. (i) uniaxial buckling and (ii) biaxial buckling. The results of both uniaxial and biaxial buckling cases are compared and depicted in the figure. From the figure (Fig. 5) it can be observed that as the scale coefficient μ increases the buckling load parameter decreases. This is in line with other previous works [21,39,55,62,63]. This decreasing nature of load parameter is due to the assimilation of small-scale effects in the DNPS. The small-scale effect reduces the stiffness of the material and hence the comparative lower buckling load. Therefore by the nonlocal elastic model, the size effects are reflected in the DNPS. Further, it is observed that DNPS are easily buckled during biaxial compression than in uniaxial compression. The buckling load parameter during biaxial compression is lesser than that of uniaxial compression at most of the scale coefficient considered. However it is worth noting that the effect of small scale is higher in buckling phenomenon of uniaxial compression than in biaxial compression.

Three different cases of biaxially compressed DNPS are considered. Case 1, case 2 and case 3 depicts the conditions (i) when both the nanoplates buckles in the out-of-phase (asynchronous) sequence ($w_1 - w_2 \neq 0$), (ii) when one of the nanoplates in DNPS is stationary ($w_2 = 0$) and (iii) when both the nanoplates buckles with in-phase (synchronous) sequence ($w_1 - w_2 = 0$), respectively. Comparing the three cases of DNPS, we observe that the buckling load parameter for case 3 (in-phase buckling behaviour) is smaller

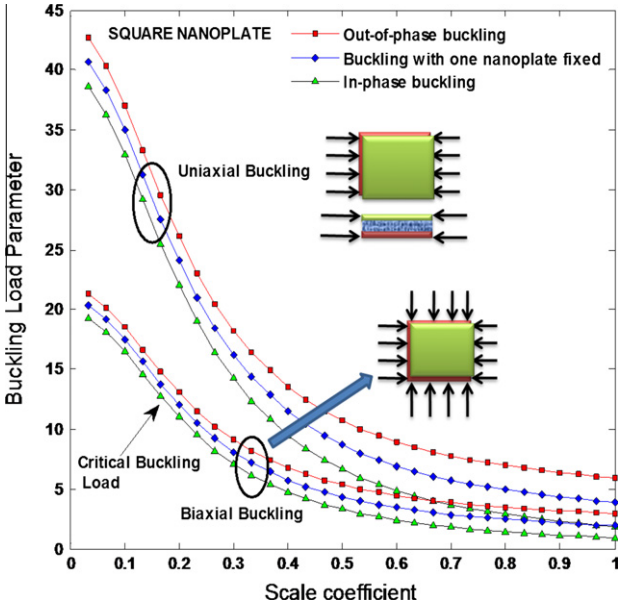

Fig. 5. Effect of nonlocal parameter or scale coefficient on buckling of square NDNPS.

than the buckling load parameter for case 1 (out of phase buckling behaviour) and case 2 (one-nanoplate fixed). In other words, the scale coefficient significantly reduces the in-phase buckling load compared to other cases considered. The low buckling load in case-3 is due to the absence of coupling effect of the spring and the two nanoplates. In addition it can be seen that the values of the buckling load parameter for case-2 (one-nanoplate fixed) is smaller than the values of the buckling load parameter for case-1 (out-of-phase buckling behaviour). For case-2 the DNPS becomes similar to the buckling behaviour characteristic of the single nanoplate with the effect of elastic medium. In case-3 (in-phase buckling behaviour) the load parameter is relatively less because the DNPS becomes independent of the effect of the spring stiffness. For case-3 the DNPS becomes similar to the buckling response of the single nanoplate without the effect of elastic medium.

In other words out-of-phase buckling is less affected by the small-scale or nonlocal effects. This out-of-phase buckling can be attributed to the fact that the coupling springs in the vibrating system dampens the nonlocal effects. In-phase buckling of coupled-system is unchangeable with increasing stiffness of springs. This is due to the in-phase buckling mode of behaviour. For in-phase type of buckling the coupled system behaves as if a single nanoplate without the effect of internal elastic medium. In other words the whole coupled system can be treated as a single nanoelement and the coupling internal structure is effect less. In summary, it should be noted that the in-phase buckling of coupled-system are more affected by small-scale effects compared to out-of-phase buckling. Also it should be noted that the above effects as discussed is less pronounced in biaxial compression than in the uniaxial compression of DNPS.

5.4. Effect of stiffness of coupling springs of DNPS

The two nanoplates are bonded by an elastic medium. The elastic medium is modelled by elastic springs. To illustrate the influence of stiffness of the springs on the buckling phenomenon of the biaxially compressed DNPS, curves have been plotted for the buckling load parameter against the scale coefficient. Spring stiffness represents the stiffness of the enclosing elastic medium (polymer resin). Similar DNPS as discussed in the earlier subsection is adopted. Different values of stiffness parameter of the coupling springs are considered. Figs. 6–9 depict the effects of stiffness of the springs on the buckling load parameter of the coupled systems. The stiffness parameter of the coupling springs are taken as $K = 5$, 10, 25 and 50, respectively. Aspect ratio (L/W) is taken as unity. Out-of-phase buckling, in-phase buckling and buckling with one nanoplate fixed is considered. Both uniaxial as well biaxial compressions of DNPS are also presented.

From the figures, it is noticed that as the stiffness parameter of the coupling springs increases the buckling load parameter increases. Considering all values of the stiffness parameter; and comparing the three cases of DNPS, it is noticed that the buckling load parameter for in-phase buckling is smaller than the buckling load parameter for out of phase buckling and one-nanoplate fixed. These different changing trends of buckling load parameter with the increasing scale coefficient for the three different cases are more amplified as the stiffness parameter of the spring's increases. Further it is also noticed from the figure that as the stiffness of the spring's increases, the curves of buckling load parameter for uniaxial compression and the biaxial compression come closer. This phenomenon is more pronounced at higher nonlocal parameter values (Fig. 9). In other words, if the bonding between two nanoplates of DNPS is stiffer and the nonlocal effect is much intense (i.e. higher nonlocal parameter), then the buckling phenomenon happens at closer values of buckling loads in uniaxial than in biaxial compression.

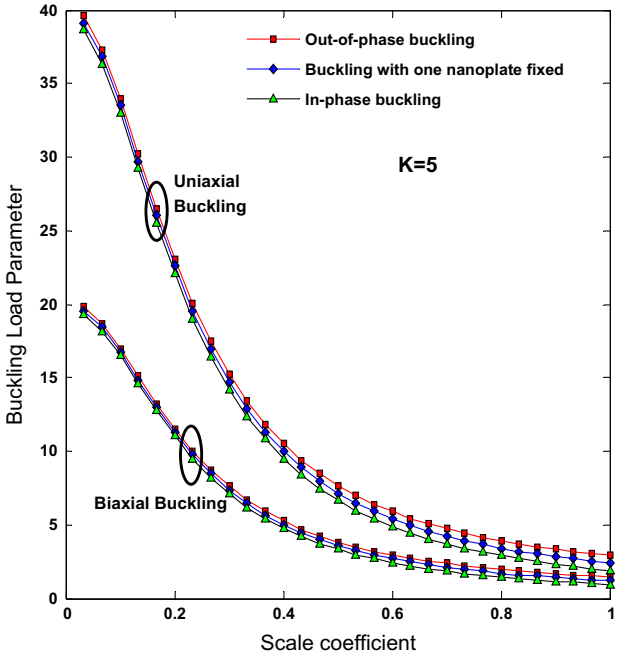

Fig. 6. Effect of scale coefficient on buckling of square DNPS for stiffness parameter $K = 5$.

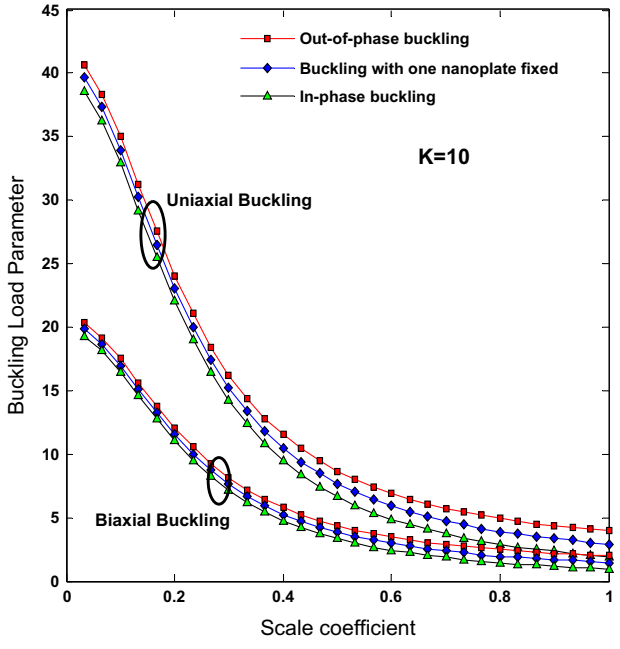

Fig. 7. Effect of scale coefficient on buckling of square DNPS for stiffness parameter $K = 10$.

5.5. Effect of aspect ratio of biaxially compressed DNPS

We illustrate here the influence of aspect ratios (L/W) of the nanoplates of DNPS on the buckling loads. Here we consider the stiffness of the bonding agent between the nanoplates (nanoplate-1 and nanoplate-2) as $K = 20$. Out-of-phase buckling, in-phase buckling and buckling with one nanoplate fixed is considered. Both uniaxial as well biaxial buckling phenomenons of DNPS are also depicted in the figure. Curves have been plotted for the

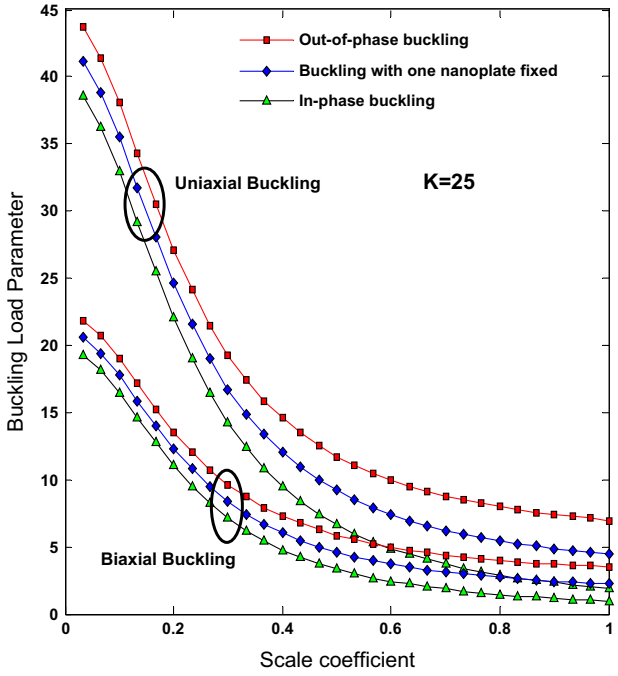

Fig. 8. Effect of scale coefficient on buckling of square DNPS for stiffness parameter $K = 25$.

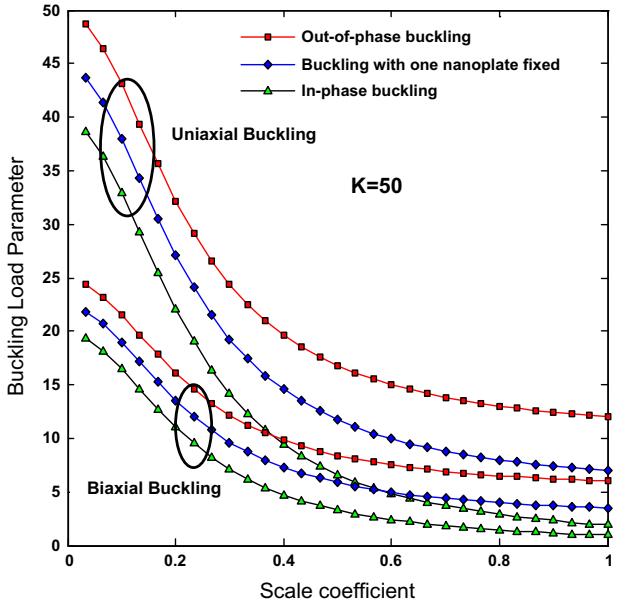

Fig. 9. Effect of scale coefficient on buckling of square DNPS for stiffness parameter $K = 50$.

buckling load parameter against the scale coefficient for different aspect ratios. Figs. 10–12 depict the effect of aspect ratio on the buckling load parameter of coupled systems. The aspect ratios are taken as $L/W = 0.5$, 1.5, and 2.0. It is observed that as the aspect ratio (L/W) of the DNPS increases, the differences among the out-of-phase buckling, in-phase buckling and buckling with one nanoplate fixed minimises. See Figs. 10 and 12. While comparing uniaxial compression and biaxial compression for DNPS of different aspect ratios, it is found that a difference between them (i.e. uniaxial and biaxial compression phenomenon) enlarges with increasing aspect ratio (L/W). This behaviour of DNPS is unlike that of increase

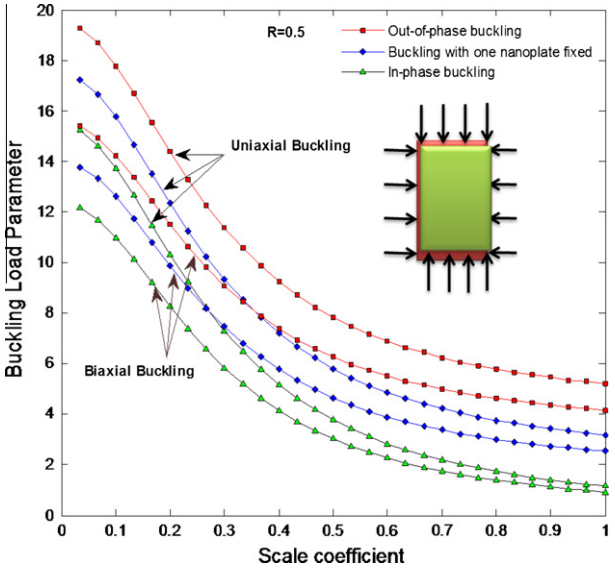

Fig. 10. Effect of scale coefficient on buckling of NDNPS for aspect ratio, $R = 0.5$.

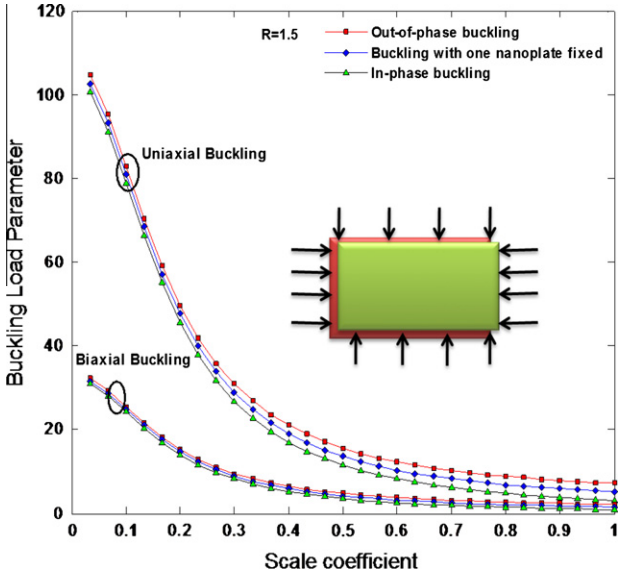

Fig. 11. Effect of scale coefficient on buckling of NDNPS for aspect ratio, $R = 1.5$.

of stiffness parameter in uniaxial and biaxial compression DNPS. Increase of stiffness parameter brings uniaxial and biaxial buckling phenomenon closer while increase of aspect ratio widen uniaxial and biaxial buckling phenomenon.

5.6. Effect of higher modes of buckling

Here we illustrate the effect of nonlocal parameter on the higher modes buckling load parameter of biaxially compressed DNPS. Higher modes of buckling in the biaxially compressed DNPS, i.e. $m = 1$, $n = 1$; $m = 1$, $n = 2$; $m = 2$, $n = 2$; and $m = 3$, $n = 3$ are depicted in Fig. 13. It should be noted that the sequential numbering of the modes i.e. $m = 1$, $n = 1$; $m = 1$, $n = 2$; $m = 2$, $n = 2$; and $m = 3$, $n = 3$ are based at $\mu = 0$. From Fig. 13 it is observed that small-scale effects are higher for higher modes of buckling, i.e.

$$m = 1, \quad n = 1 < m = 1, \quad n = 2 < m = 2, \quad n = 2 < m = 3, \quad n = 3$$

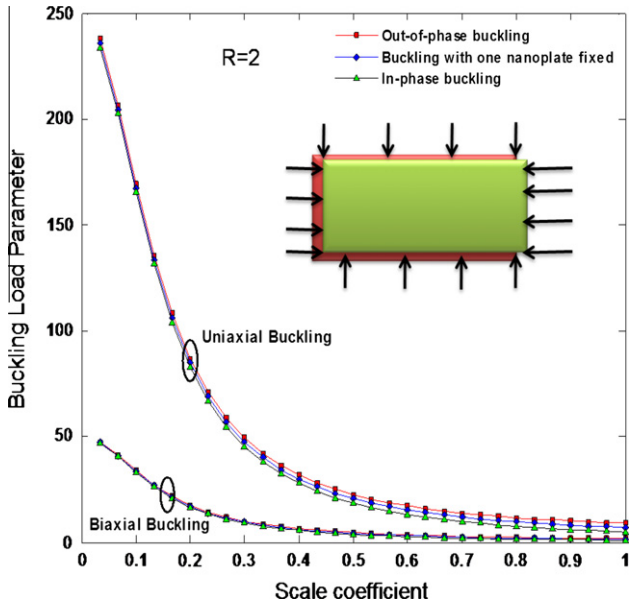

Fig. 12. Effect of scale coefficient on buckling of NDNPS for aspect ratio, $R = 2$.

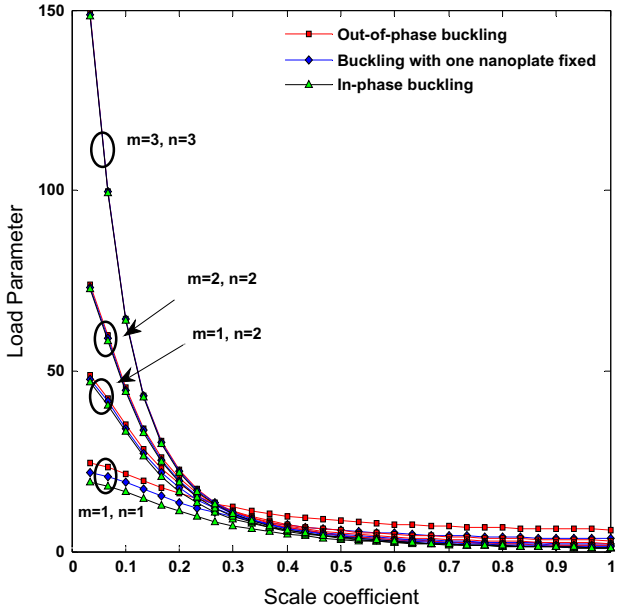

Fig. 13. Effect of scale coefficient on bi-axial buckling of NDNPS for higher modes.

This is similar to effect in uniaxial buckling phenomenon [55,66]. Further it is important to note that with increasing modes of buckling, the difference among the (i) out-of-phase (asynchronous) sequence ($w_1 - w_2 \neq 0$), (ii) in-phase (synchronous) sequence($w_1 - w_2 = 0$) of buckling and (iii) one nanoplate stationary reduces. For modes $m = 3$, $n = 3$, it could be see that this difference is negligible.

5.7. Effect of compression ratio on bi-axially compressed DNPS

The effect of different biaxial compression ratio (δ) on DNPS is also studied. Different biaxial compression ratio would impart different buckling phenomenon. The biaxial compression ratios (δ) used are $\delta = 0, 0.5, 1.0, 1.5,$ and 2.0. The compression ratio $\delta = 0$ represents uniaxial compression, whereas $\delta = 1$ represents uniform biaxial compression. Fig. 14 depicts the variation of load parameter

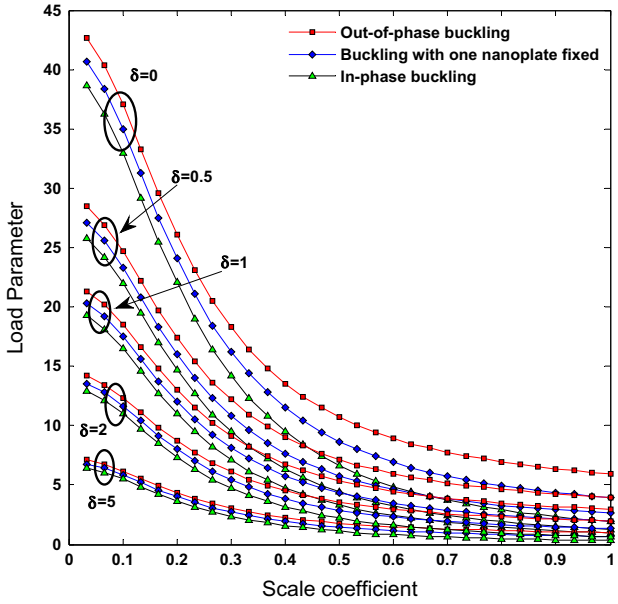

Fig. 14. Effect of scale coefficient on bi-axial buckling of NDNPS for higher compression ratios.

with the change of nonlocal parameter for different compression ratios. For higher compression ratios (δ) it is observed that difference among the (i) out-of-phase (asynchronous) sequence ($w_1 - w_2 \neq 0$), (ii) in-phase (synchronous) sequence ($w_1 - w_2 = 0$) of buckling and (iii) one nanoplate stationary reduces. Compare curves for $\delta = 0.5$ and $\delta = 5.0$. Further it is important to note that the values of buckling load parameter drops drastically with increase of scale coefficient for uniaxial compression than in biaxial compression.

The present work depicts a quantitative analysis. It should be noted that we have assumed that the interlayer distance would have no influence on the buckling even with the same value of the stiffness parameter K. This is because we have focused on the same-phase and anti-phase behaviour of the two one atomic layer thickness nanoplates (graphene).

The present study could be used for the fast prediction of stability behaviour of square and rectangular nanoplates such as of graphene sheets. This present double-nanoplate-theory can be extended to plates of small scale for various shapes, such as circular nanoplates and skew nanoplates. The specific value of nonlocal parameter of DNPS is yet unknown. In the present work we have considered a range of nonlocal parameter. Further the molecular dynamics simulation of the present work to determine the optimised nonlocal parameter is still unavailable in literature and represents a scope of future works.

6. Conclusion

In this article we illustrate small scale effect on the buckling analysis of biaxial compressed DNPS within the framework of Eringen's nonlocal elasticity. Nonlocal plate model is utilised. Out-of-phase (asynchronous), in-phase (synchronous) buckling, and buckling phenomenon one nanoplate stationary are considered for the DNPS. An analytical method is introduced for determining buckling load of biaxially compressed DNPS. Explicit closed-form expressions for buckling load are derived for the case when all four ends are simply-supported. Effects of (i) small (nano) scale, (ii) stiffness of coupling springs, (iii) aspect ratios, (iv) higher modes number, and (v) different compression ratios on buckling loads of DNPS are presented. Both uniaxial compression and biaxial compression

aspects are illustrated. The study highlights that that small scale effects contribute significantly to the buckling behaviour of biaxially compressed and cannot be neglected. The small-scale effects in biaxially compressed are higher with increasing values of nonlocal parameter for the case of synchronous modes of buckling than in the asynchronous modes of buckling. The nonlocal buckling solutions are always smaller than the local counterpart for both uniaxial and biaxial compression. Further buckling load decrease with increase of nonlocal parameter value. Increase of stiffness parameter brings uniaxial and biaxial buckling phenomenon closer while increase of aspect ratio widen uniaxial and biaxial buckling phenomenon. Higher buckling modes are subjected to higher nonlocal effects. This work may provide an analytical scale-based nonlocal approach which could serve as the starting point for further investigation of more complex *n*-nanoplates systems undergoing instability.

References

[1] Han T, He P, Wang J, Wu A. Molecular dynamics simulation of a single graphene sheet under tension. New Carbon Mater 2010;25:261.
[2] Margono C, Zhang Q, Goebl J, Yin Y. Synthesis of gold nanoplates using polyacrylic acid. Abstr Pap Am Chem Soc 2011;241.
[3] Liu X, Peng X, Yang Z, Li M, Zhou L. Linear and nonlinear optical properties of micrometer-scale gold nanoplates. Chin Phys Lett 2011;28.
[4] Liu H, Yang Q. Feasible synthesis of etched gold nanoplates with catalytic activity and SERS properties. CrystEngComm 2011;13:5488.
[5] Swarnavalli G, Joseph V, Kannappan V, Roopsingh D. A simple approach to the synthesis of hexagonal-shaped silver nanoplates. J Nanomater 2011.
[6] Goebl J, Zhang Q, Yin Y. Growth of silver nanoplates containing gold nanorings. Abstr Pap Am Chem Soc 2011;241.
[7] Illy B, Shollock B, MacManus-Driscoll J, Ryan M. Electrochemical growth of ZnO nanoplates. Nanotechnology 2005;16:320.
[8] Pacile D, Meyer J, Girit C, Zettl A. The two-dimensional phase of boron nitride: few-atomic-layer sheets and suspended membranes. Appl Phys Lett 2008;92.
[9] Xu L, Zhan J, Hu J, Bando Y, Yuan X, Sekiguchi T, et al. High-yield synthesis of rhombohedral boron nitride triangular nanoplates. Adv Mater 2007;19:2141.
[10] Moon J, Gaskill D. Graphene: its fundamentals to future applications. IEEE Trans Microw Theory Tech 2011;59:2702.
[11] Xu Y, Guo Z, Chen H, Yuan Y, Lou J, Lin X, et al. In-plane and tunneling pressure sensors based on graphene/hexagonal boron nitride heterostructures. Appl Phys Lett 2011;99.
[12] Rogers G, Liu J. Graphene actuators: quantum-mechanical and electrostatic double-layer effects. J Am Chem Soc 2011;133:10858.
[13] Zhang Q, Lu Y, Xing H, Koester S, Koswatta S. Scalability of atomic-thin-body (ATB) transistors based on graphene nanoribbons. IEEE Electron Dev Lett 2010;31:531.
[14] Ryzhii M, Satou A, Ryzhii V, Otsuji T. High-frequency properties of a graphene nanoribbon field-effect transistor. J Appl Phys 2008;104.
[15] Sima M, Enculescu I, Sima A. Preparation of graphene and its application in dye-sensitized solar cells. Optoelectron Adv Mater – Rapid Commun 2011;5:414.
[16] Hsieh C, Yang B, Lin J. One- and two-dimensional carbon nanomaterials as counter electrodes for dye-sensitized solar cells. Carbon 2011;49:3092.
[17] Das S, Sudhagar P, Verma V, Song D, Ito E, Lee S, et al. Amplifying charge-transfer characteristics of graphene for triiodide reduction in dye-sensitized solar cells. Adv Funct Mater 2011;21:3729.
[18] Yang L, Zhang L, Webster T. Carbon nanostructures for orthopedic medical applications. Nanomedicine 2011;6:1231.
[19] Morin S, Forticaux A, Bierman M, Jin S. Screw dislocation-driven growth of two-dimensional nanoplates. Nano Lett 2011;11:4449.
[20] Murmu T, Adhikari S. Non local vibration of bonded double-nanoplate-systems. Compos Part B: Eng 2011;42:1901.
[21] Shi J, Ni Q, Lei X, Natsuki T. Nonlocal elasticity theory for the buckling of double-layer graphene nanoribbons based on a continuum model. Comput Mater Sci 2011;50:3085.
[22] Liu M, Yin X, Zhang X. Double-layer graphene optical modulator. Nano Lett 2012;12:1482.
[23] Lin Q, Rosenberg J, Chang D, Camacho R, Eichenfield M, Vahala K, et al. Coherent mixing of mechanical excitations in nano-optomechanical structures. Nat Photonics 2010;4:236.
[24] Murmu T, Sienz J, Adhikari S, Arnold C. Nonlocal buckling behavior of bonded double-nanoplate-systems. J Appl Phys 2011;110.
[25] Pouresmaeeli S, Fazelzadeh FA, Ghavanloo E. Exact solution for nonlocal vibration of double-orthotropic nanoplates embedded in elastic medium. Compos Part B: Eng 2012 [corrected proof].
[26] Beni Y, Koochi A, Abadyan M. Theoretical study of the effect of Casimir force, elastic boundary conditions and size dependency on the pull-in instability of beam-type NEMS. Phys E – Low-Dimens Syst Nanostruct 2011;43:979.
[27] Akgoz B, Civalek O. Strain gradient elasticity and modified couple stress models for buckling analysis of axially loaded micro-scaled beams. Int J Eng Sci 2011;49:1268.
[28] Kong S, Zhou S, Nie Z, Wang K. Static and dynamic analysis of micro beams based on strain gradient elasticity theory. Int J Eng Sci 2009;47:487.
[29] Kahrobaiyan M, Asghari M, Rahaeifard M, Ahmadian M. Investigation of the size-dependent dynamic characteristics of atomic force microscope microcantilevers based on the modified couple stress theory. Int J Eng Sci 2010;48:1985.
[30] Eringen A. On differential-equations of nonlocal elasticity and solutions of screw dislocation and surface-waves. J Appl Phys 1983;54:4703.
[31] Wang Q. Wave propagation in carbon nanotubes via nonlocal continuum mechanics. J Appl Phys 2005;98.
[32] Wang Q, Varadan V. Vibration of carbon nanotubes studied using nonlocal continuum mechanics. Smart Mater Struct 2006;15:659.
[33] Simsek M. Vibration analysis of a single-walled carbon nanotube under action of a moving harmonic load based on nonlocal elasticity theory. Phys E – Low-Dimens Syst Nanostruct 2010;43:182.
[34] Li C, Lim C, Yu J, Zeng Q. Transverse vibration of pre-tensioned nonlocal nanobeams with precise internal axial loads. Sci China – Technol Sci 2011;54:2007.
[35] Besseghier A, Tounsi A, Houari M, Benzair A, Boumia L, Heireche H. Thermal effect on wave propagation in double-walled carbon nanotubes embedded in a polymer matrix using nonlocal elasticity. Phys E – Low-Dimens Syst Nanostruct 2011;43:1379.
[36] Benzair A, Tounsi A, Besseghier A, Heireche H, Moulay N, Boumia L. The thermal effect on vibration of single-walled carbon nanotubes using nonlocal Timoshenko beam theory. J Phys D – Appl Phys 2008:41.
[37] Heireche H, Tounsi A, Benzair A, Mechab I. Sound wave propagation in single-walled carbon nanotubes with initial axial stress. J Appl Phys 2008;104.
[38] Heireche H, Tounsi A, Benzair A, Maachou M, Bedia E. Sound wave propagation in single-walled carbon nanotubes using nonlocal elasticity. Phys E – Low-Dimens Syst Nanostruct 2008;40:2791.
[39] Babaei H, Shahidi A. Small-scale effects on the buckling of quadrilateral nanoplates based on nonlocal elasticity theory using the Galerkin method. Arch Appl Mech 2011;81:1051.
[40] Kiani K. Small-scale effect on the vibration of thin nanoplates subjected to a moving nanoparticle via nonlocal continuum theory. J Sound Vib 2011;330:4896.
[41] Challamel N, Lanos C, Casandjian C. Plastic failure of nonlocal beams. Phys Rev E 2008;78.
[42] Aghababaei R, Reddy J. Nonlocal third-order shear deformation plate theory with application to bending and vibration of plates. J Sound Vib 2009;326:277.
[43] Lim C, Yang Q. Nonlocal thermal-elasticity for nanobeam deformation: exact solutions with stiffness enhancement effects. J Appl Phys 2011;110.
[44] Heireche H, Tounsi A, Benhassaini H, Benzair A, Bendahmane M, Missouri M, et al. Nonlocal elasticity effect on vibration characteristics of protein microtubules. Phys E – Low-Dimens Syst Nanostruct 2010;42:2375.
[45] Amara K, Tounsi A, Mechab I, Adda-Bedia E. Nonlocal elasticity effect on column buckling of multiwalled carbon nanotubes under temperature field. Appl Math Model 2010;34:3933.
[46] Artan R, Tepe A. Nonlocal effects in curved single-walled carbon nanotubes. Mech Adv Mater Struct 2011;18:347.
[47] Simsek M. Non local effects in the forced vibration of an elastically connected double-carbon nanotube system under a moving nanoparticle. Comput Mater Sci 2011;50:2112.
[48] Hsu J, Lee H, Chang W. Longitudinal vibration of cracked nanobeams using nonlocal elasticity theory. Curr Appl Phys 2011;11:1384.
[49] Simsek M. Forced vibration of an embedded single-walled carbon nanotube traversed by a moving load using nonlocal Timoshenko beam theory. Steel Compos Struct 2011;11:59.
[50] Tounsi A, Heireche H, Berrabah H, Benzair A, Boumia L. Effect of small size on wave propagation in double-walled carbon nanotubes under temperature field. J Appl Phys 2008;104.
[51] Simsek M. Dynamic analysis of an embedded microbeam carrying a moving microparticle based on the modified couple stress theory. Int J Eng Sci 2010;48:1721.
[52] Wang Q, Wang C. The constitutive relation and small scale parameter of nonlocal continuum mechanics for modelling carbon nanotubes. Nanotechnology 2007;18.
[53] Ansari R, Rouhi H, Sahmani S. Calibration of the analytical nonlocal shell model for vibrations of double-walled carbon nanotubes with arbitrary boundary conditions using molecular dynamics. Int J Mech Sci 2011;53:786.
[54] Wang Q, Liew K. Application of nonlocal continuum mechanics to static analysis of micro- and nano-structures. Phys Lett A 2007;363:236.
[55] Aksencer T, Aydogdu M. Levy type solution method for vibration and buckling of nanoplates using nonlocal elasticity theory. Phys E – Low-Dimens Syst Nanostruct 2011;43:954.
[56] Aydogdu M. Axial vibration of the nanorods with the nonlocal continuum rod model. Phys E – Low-Dimens Syst Nanostruct 2009;41:861.
[57] Aydogdu M, Filiz S. Modeling carbon nanotube-based mass sensors using axial vibration and nonlocal elasticity. Phys E – Low-Dimens Syst Nanostruct 2011;43:1229.
[58] Ece M, Aydogdu M. Nonlocal elasticity effect on vibration of in-plane loaded double-walled carbon nano-tubes. Acta Mech 2007;190:185.

[59] Filiz S, Aydogdu M. Axial vibration of carbon nanotube heterojunctions using nonlocal elasticity. Comput Mater Sci 2010;49:619.
[60] Malekzadeh P, Setoodeh A, Beni A. Small scale effect on the free vibration of orthotropic arbitrary straight-sided quadrilateral nanoplates. Compos Struct 2011;93:1631.
[61] Wang Y, Li F, Kishimoto K. Flexural wave propagation in double-layered nanoplates with small scale effects. J Appl Phys 2010;108.
[62] Murmu T, Pradhan S. Buckling of biaxially compressed orthotropic plates at small scales. Mech Res Commun 2009;36:933.
[63] Pradhan S, Murmu T. Small scale effect on the buckling of single-layered graphene sheets under biaxial compression via nonlocal continuum mechanics. Comput Mater Sci 2009;47:268.
[64] Ansari R, Sahmani S, Arash B. Nonlocal plate model for free vibrations of single-layered graphene sheets. Phys Lett A 2010;375:53.
[65] Ansari R, Arash B, Rouhi H. Vibration characteristics of embedded multi-layered graphene sheets with different boundary conditions via nonlocal elasticity. Compos Struct 2011;93:2419.
[66] Pradhan S, Murmu T. Small scale effect on the buckling analysis of single-layered graphene sheet embedded in an elastic medium based on nonlocal plate theory. Phys E – Low-Dimens Syst Nanostruct 2010;42:1293.
[67] Pradhan S, Phadikar J. Small scale effect on vibration of embedded multilayered graphene sheets based on nonlocal continuum models. Phys Lett A 2009;373:1062.
[68] Narendar S, Gopalakrishnan S. Spectral finite element formulation for nanorods via nonlocal continuum mechanics. J f Appl Mech – Trans ASME 2011;78.
[69] Shen L, Shen H, Zhang C. Nonlocal plate model for nonlinear vibration of single layer graphene sheets in thermal environments. Comput Mater Sci 2010;48:680.